REGULAR ARTICLE

blood VTH
vessels, thrombosis & hemostasis

Murine thrombus organization limits access to high platelet activation states while supporting platelet recruitment

Sung W. Rhee,[1,*] Irina D. Pokrovskaya,[2,*] Kelly K. Ball,[2] Michael W. Webb,[2] Jeffrey A. Kamykowski,[2] Maria A. Aronova,[3] Richard D. Leapman,[3] Elizabeth R. Driehaus,[4] Erich S. Franz,[4] Sidney W. Whiteheart,[4] and Brian Storrie[2]

[1]Department of Pharmacology and Toxicology and [2]Department of Physiology and Cell Biology, University of Arkansas for Medical Sciences, Little Rock, AR; [3]Laboratory of Cellular Imaging and Macromolecular Biophysics, National Institute of Biomedical Imaging and Bioengineering, National Institutes of Health, Bethesda, MD; and [4]Department of Molecular and Cellular Biochemistry, University of Kentucky College of Medicine, Lexington, KY

Key Points

- Exposure of highly activated platelet surfaces to intravascular factors peaks after bleeding cessation.
- Modulating exposure of highly activated platelet surfaces to circulating coagulation factors is a potential target for limiting thrombosis.

Platelet aggregation at sites of vascular injury is essential for hemostasis. However, the mechanisms that prevent excessive clot growth are not fully understood. In the prevailing "core and shell" model, based largely on small vessel injury studies, a central core of highly activated platelets is surrounded by a limited signal intensity shell of less activated, minimally degranulated platelets. Recent reports, especially in mouse models of profuse bleeding, suggest thrombus architecture and platelet activation states are more heterogeneous than the binary core and shell model proposes. Here, we performed high-resolution morphometric mapping of individual platelet activation states in mouse jugular vein and femoral artery puncture wound thrombi, using serial block face scanning electron microscopy and wide-area transmission electron microscopy. Manually annotated images were analyzed at multiple time points, revealing initial, 1-minute, near-complete intermixing of platelet activation states with no distinct core of highly activated platelets. At 5 minutes, highly activated, degranulated platelets became concentrated along the interior surfaces of vaulted thrombus structures. At 20 minutes, platelet numbers decreased and distinct clustering of degranulated, highly activated platelets was observed within central portions of the intravascular platelet-rich crown, limiting their access to the circulation. Deletion of the α-granule vesicle-soluble N-ethylmaleimide-sensitive factor attachment protein receptor, vesicle associated membrane protein 8, increased both the frequency and clustering of highly activated platelets. Similar patterns were observed in femoral artery wounds. We conclude that thrombus organization is more complex than previously recognized and provide evidence that progressive structural changes help limit procoagulant surface exposure and thrombus growth during hemostasis after puncture wounding.

Introduction

Within the circulation, the platelet functions as a surveillance cell that is recruited to sites of vascular damage, for example, damaged endothelial cells or exposed extracellular matrix in the case of a

Submitted 4 August 2025; accepted 22 January 2026; prepublished online 23 February 2026. https://doi.org/10.1016/j.bvth.2026.100154.

*S.W.R. and I.D.P. are joint first authors.

Image sets reported in this article have been deposited in the Electron Microscopy Public Image Archive (EMPIAR) (https://www.ebi.ac.uk/empiar/; EMPIAR identity accession code 10785, September 2021). Additional data sets will be deposited and made publicly available as raw images upon acceptance of this manuscript.

Image sets are available from the corresponding author, Brian Storrie (storriebrian@uams.edu), on request.

The full-text version of this article contains a data supplement.

puncture wound.[1,2] The initially recruited platelet is discoid-shaped and bound by adhesion receptors that mediate its tethering to proteins such as collagen and von Willebrand factor.[3-10] These platelets are rich in platelet secretory organelles including dense granules and α-granules, and virtually indistinguishable from circulating platelets.[10] Further platelet recruitment and molecular interactions lead to the progressive formation of a platelet-rich aggregate, a thrombus. During this process, external, agonist-induced activation of platelet cell surface proteins such as PAR receptors and paracrine activation of ADP/thromboxane-sensitive P2Yx receptors result in the accumulation of platelets in various activation states.[11-13] They include granule-rich, degranulated, loosely or tightly adherent platelets, rich in cell surface exposed phosphatidylserine and P-selectin, an α-granule membrane protein.[14-16] How the resulting thrombus structure is organized in larger models such as a puncture wound to the jugular vein[17,18] or femoral artery of mice vs smaller models such as arterioles[19] remains an open question that is fundamental to distinguishing between hemostatic and thrombotic responses.

Much of our knowledge of thrombus formation comes from the study of small diameter, 20- to 40-μm arterioles, for example, the cremaster arterioles of mice,[1] a model of thromboinflammation.[20,21] Injury is nonpenetrating and underlying collagen-rich adventitia is not exposed. Because of the small arteriole size and their easy exposure, the model has been a favorite for intravital microscopy analysis.[19,22] Overall, the outcomes point to binary differences in platelet activation state between a damage-proximal "core" of highly activated, degranulated, tightly adherent platelets and a distal "shell" of loosely adherent, granulated platelets with a low-activation state.[23] Inhibitor experiments indicate diffusion-limited signaling with thrombin, a strong activator, being the major agonist in the core and ADP and thromboxane, released locally by low-activation-state platelets being the major signaling agonists in the shell.[13] With the recent application of volume electron microscopy (vEM) to yield 3-dimensional (3D) platelet imaging within cremaster thrombi, consideration has been given to a gradient analysis of the distribution of platelet activation state as signal intensity radiates out spatially from the site of laser damage.[21] Based on this evidence, the authors propose a radial formation model in which signals fan radially outward from the thrombus core.

Work with profuse bleeding models such as the mouse jugular vein puncture wound, ~250-μm hole, may well present a more complex set of outcomes. On the one hand, based on 2-photon light microscopy and scanning electron microscopy (SEM) of thrombus surface features, the profuse bleeding puncture wound thrombus has been proposed to be an extension of the core and shell framework.[17] In contrast, data from vEM approaches indicate platelets in the profuse bleeding example are found in multiple, nonbinary microenvironments.[10,18,24] At near-nanometer resolution, the primary puncture wound hemostatic clot appears to be initiated by nucleated platelet attachment to the exposed, collagen-rich adventitia,[18] which leads to the formation of columnar platelet aggregates that form a vaulted thrombus structure, which is capped from the extravascular side to produce bleeding cessation.[18] These unexpected patterns of platelet aggregation raise the possibility of novel structural determinants and signaling patterns within the primary puncture wound thrombus.

We used single-platelet, morphometric mapping of platelet activation state,[24] to determine the kinetics of high platelet activation state exposure and to infer from 2D gradients, platelet activation signaling axes in a mouse puncture wound model. Detailed, multiple time point characterization of platelet activation 2D patterning revealed a progressive, secretion-dependent remodeling of thrombus structure that limited access to high-activation platelet surfaces. Contrary to the expectations of an extended core and shell model, inferred high intensity signaling effects appeared to propagate short distances, $\leq$5 μm, from both the exposed adventitial interface and intravascularly exposed thrombus surfaces, indicating a second, nonadventitial signaling axis. Detailed profiling of platelet activation revealed the absence of significant gradients in platelet activation within early, 1-minute postpuncture wound thrombi, prebleeding cessation. In brief, the puncture wound showed little to no evidence of being structured initially around a high-activation core from which signaling gradients propagated. We conclude that our structural evidence provides a novel understanding of intrathrombus organization and inferred signaling gradients in a physiologically important example of primary hemostasis, the profuse bleeding puncture wound.

Materials and methods

Mice and reagents

C57BL/6 mice and their derivatives were used, as approved by the institutional animal care and use committee. Their use and reagents have been described elsewhere.[10,18,25] Vesicle associated membrane protein 8 (VAMP8)-knockout (KO; VAMP8$^{-/-}$) mice have been described previously.[26]

Puncture wounds

Jugular vein puncture wounds were performed with a 30-gauge syringe needle with a nominal diameter of 312 μm.[10,18,25] Femoral artery puncture wounds were done with a 33-gauge syringe needle with a diameter of 210 μm.

Thrombus preparation and electron microscopy

Wide-area (WA) transmission electron microscopy (TEM) and supporting serial block face (SBF)–SEM were performed as previously described.[10,18,25] WA-TEM micrographs, pixel size 3.185 nm, 500 to 900 individual frames at 4 × 10^3 by 4 × 10^3 pixels, were montaged to give WA-TEM cross-sections of full thrombus width. The sample preparation procedures used for WA-TEM emphasize membrane clarity vs such cellular components as RNA-rich ribosomes, a choice appropriate for the goals of these experiments.

Data sets

The raw images of 2 of the 1- and 20-minute postpuncture thrombi (WA-TEM, 3.185 nm pixel size) were published previously at a low zoom.[10,18] Additional data sets were generated to increase the robustness of our analysis. All mapping analysis, resulting quantitative analysis, and mapping imagery are unique and original to this study.

Manually annotated platelet activation state mapping and nearest neighbor analysis (ground truth analysis)

Images were manually annotated at a pixel size between 12 and 15 nm and analyzed as previously described.[24] Statistical

significance of the tabulated outcomes was calculated as previously published.[24] Platelet activation gradient histograms were plotted in x- and y-axes for the individual thrombus examples using the respective "csv" classifications and binning platelet activation state counts across a 20-μm wide band in the x-axis or y-axis. A separate supplemental Materials Excel spreadsheet illustrates how calculations were done.

Results

Analyzing platelet activation states in 2D

Previously, we used SBF-SEM supplemented by limited WA-TEM to render full thrombus volumes of jugular vein, puncture wound thrombi.[10,18,25] These experiments provided preliminary evidence that highly activated platelets in 1- and 5-minute samples were enriched in a thin layer at the exposed adventitial interface and the surface of platelet-free vaults. By 20 minutes after puncture, vaults had shrunk, and thrombus volume decreased relative to 5 minutes ($P < .05$).[10] Because of the relatively low resolution of these SBF-SEM–based experiments (100 nm typical pixel size), we could not define the activity states of individual platelets within the forming thrombi and hence could make only general inferences about platelet morphology, putative platelet activation class distribution, and how signaling might change locally within the forming thrombi.

We have now used WA-TEMs imaged at 3.185-nm pixel size and hence have been able to stratify individual platelets into 5 classes chosen to emphasize low- to high-activation traits based on morphology: discoid (blue); rounded, granulated (cyan); partially degranulated (green); cytosol-rich, degranulated (α-granule negative) and cytosol rich, (yellow); and procoagulant, devoid of internal contents (red) (Figure 1). These classes correspond to observed states in our previous work with stimulated platelets in suspension.[27] Our distinctions based on 2D platelet morphology are validated against prediction in Figure 2 and supplemental Figures 1-4. We predict that if the activation state distinctions are physiologically based, then as thrombus structure evolves over time, increased spatial stratification of platelet activation states should occur. That is indeed the case at 1 vs 5 and 20 minutes after puncture. Functionally, the discoid-shaped platelets (blue) correspond to newly recruited platelets that have not yet begun to show morphologically distinct activation traits. The shape changed, granulated to partially degranulated platelets (cyan and green, respectively), make up the bulk of the platelets within the

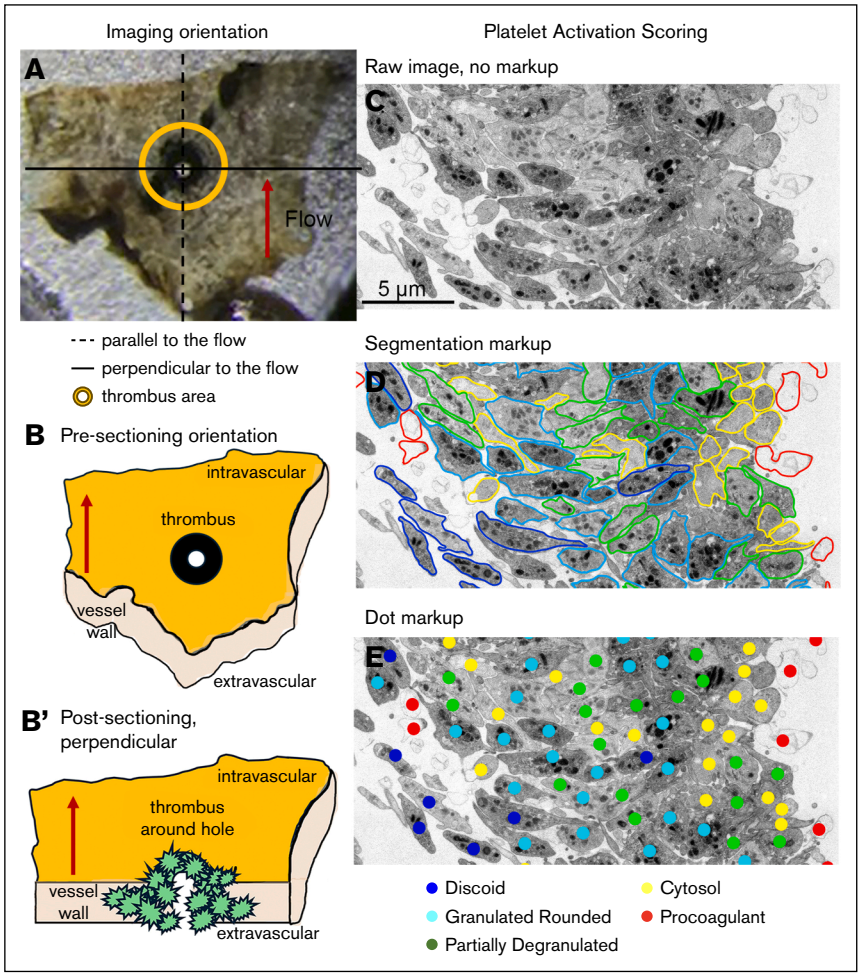

Figure 1. Sample preparation for WA-TEM and manual annotations of platelet activation states. (A-B′) Sample preparation and visual definition of parallel and perpendicular to flow sectioning. (C-E) Illustration of activation state annotation protocol from raw image to fully annotated image. Note that the manual annotator adjusts for platelet-to-platelet variation in staining intensity. Frames D and E are annotated versions of frame C, and hence the scale bar in frame C applies to frames D and E.

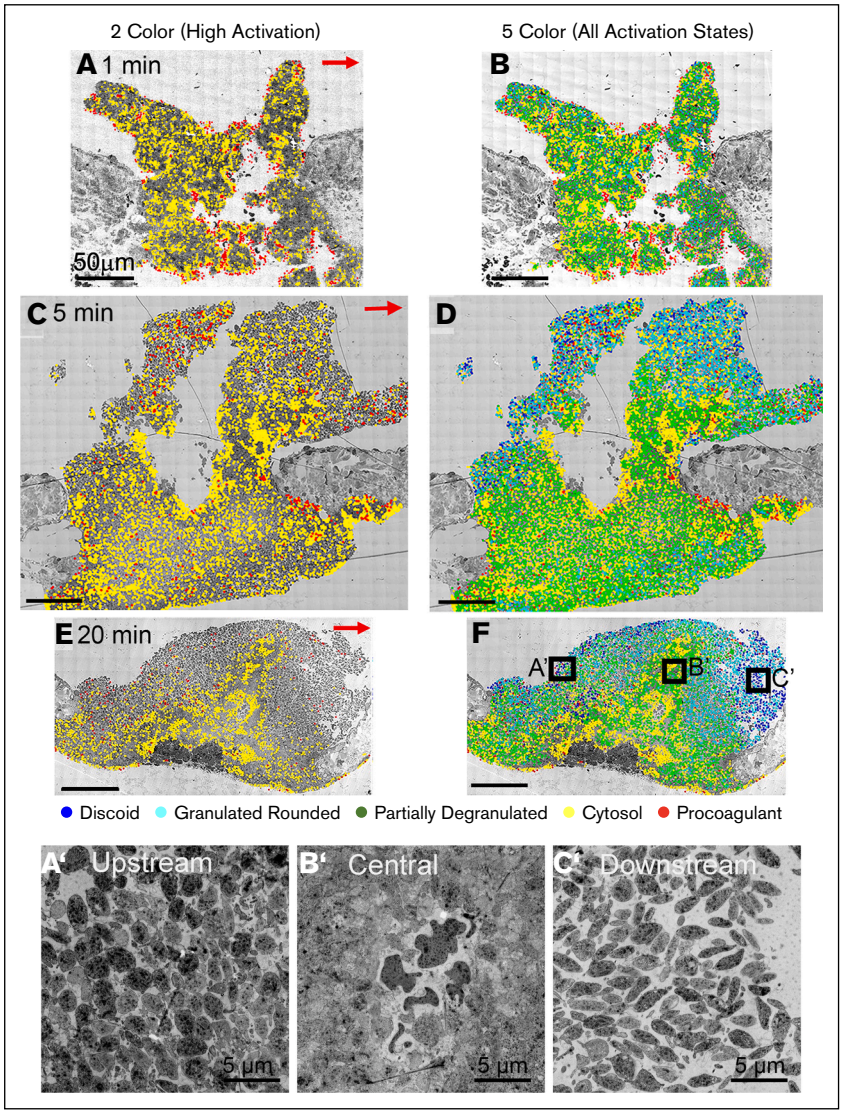

Figure 2. Annotated images of platelet activation state distribution in jugular vein at 1, 5, and 20 minutes after puncture wounding. The images were taken parallel to flow. (A-F) Time series, WA-TEM images annotated, left column: high-activation states (yellow and red); right column: all 5 activation states (+blue, cyan, and green). (F) Boxes mark regions of interest shown at higher magnification in panels A′-C′. Arrows in the 5-color images indicate the plane chosen for horizontal and vertical histogram profiling of platelet activation state (see supplemental Figure 1). For additional analysis examples, parallel and perpendicular to flow at each time point, see supplemental Figures 2-4.

thrombus. Functionally, their adhesion, presumably integrin-dependent, appears to be their most important property. Finally, the degranulated to cytosol-free platelets (yellow and red) are highly activated morphologically with the cytosol-free platelets being presumptive procoagulant platelets. No effort was made to quantify dense granules as their vEM incidence in C57BL/6 mice at 2.4 per platelet[28] is too small to make quantitative comparisons that are meaningful within 2D, single-plane sections.

Postpuncture, jugular vein wound thrombi show a progressive stratification of high-activation-state platelets

Three individual puncture wounds each were imaged at 1, 5, and 20 minutes after jugular vein puncture. Because jugular vein bleeding times are short, 1.1 minutes,[24] the initial time point is just before bleeding cessation. As shown in Figure 2 (see also supplemental Figures 2-4 for additional examples), there was a progressive kinetic shift in the distribution of highly activated, cytosol-positive, degranulated platelets (yellow and red, "hot" colors) relative to other activation states (blue, cyan, and green, "cold" colors, low to moderate activation). The highest activation class, relatively rare procoagulant, devoid of cytosol and all organelles (red) was located adjacent to exposed adventitia or on exposed peripheral surfaces, particularly those of internal vaults within the forming thrombus. In contrast, cytosol-rich, degranulated platelet profiles (yellow) were much more abundant and found over much of the forming, 1-minute thrombus (Figure 2A-B). Discoid platelets (blue) were especially numerous on the hole exposed surfaces of the cross-section cut perpendicular to flow (supplemental Figure 2). As shown in Figure 2A-B, moderate activation platelets, with varying degrees of granulation (cyan and green), were found over most of the 1-minute thrombi. In total, 53% of the platelets scored were granule-positive, rounded, adherent platelets. The higher activation at the peripheral areas of the 1-minute thrombi was consistent with previous qualitative

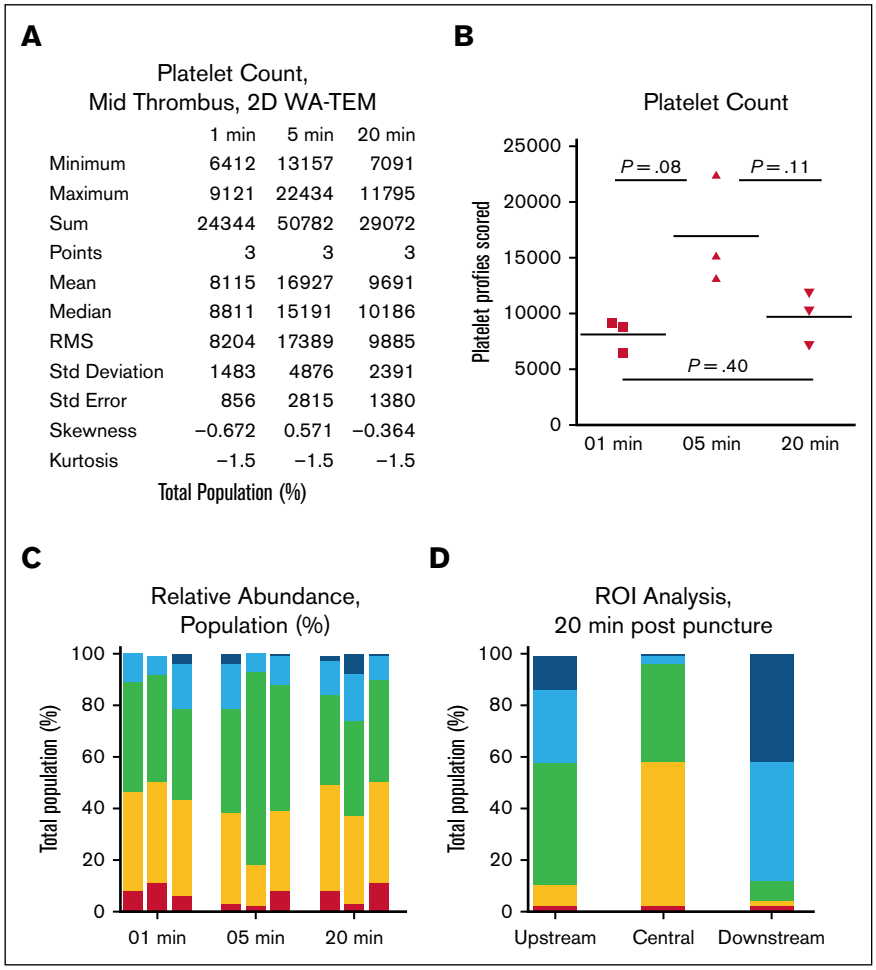

Figure 3. Quantitative analysis of the distribution of platelet activation states in jugular thrombi at 1, 5, and 20 minutes after puncture. (A) Statistical summary. (B) Comparative platelet abundance in the scored mid–cross-section examples (3 each). A *P* value <.05 is statistically significant for thrombus volume at each time point, as previously published.[10] (C) Relative total abundance of each platelet activation state at the individual time points. Note that the total abundance of the activation states does not significantly vary across time points. (D) ROI analysis at 20 minutes after puncture, shows significant variation from region to region in a pattern that illustrates important differences that correlate with flow. Past lower resolution analysis predicts greater recruitment of discoid platelets (blue) to the downstream side of a thrombus.[10,18] ROI, regions of interest; Std, standard.

results.[18] To provide a high granularity, quantitative assessment, we profiled individual activation state distributions relative to the adventitia, horizontal x-axis and a vertical y-axis (arrowheads, Figure 2B; supplemental Figure 1). In sum, the 1-minute postpuncture mapping as quantified in the histogram analysis (supplemental Figure 1), points to a mixed "salt and pepper" distribution of major activation classes.

Locally significant examples of self-association were seen for discoid platelets within the puncture hole or, more broadly, that of rounded, fully granulated platelets, and procoagulant platelets proximal to the exposed adventitia. These results are consistent with the "tethered capture and activate" model of initial platelet recruitment in which initial adherence at the collagen-rich adventitia produces a procoagulant state.[10] Repeated platelet recruitment within the puncture hole then leads to subsequent activation that in the 1-minute postpuncture case often does not progress past partial degranulation as indicated by the morphologically identifiable large granule class, α-granules. In conclusion, these results provide little to no support for a puncture wound core and shell model.

At 5 minutes after puncture, the thrombus was expected to show an intravascular crown with typically extensive vaults and substantial extravascular platelet accumulation that caps the puncture hole and prevents further bleeding.[10,18] The images in Figure 2C-D are consistent with these expectations. A substantial extravascular cap was present in all 3 examples (Figure 2; supplemental Figure 3). Rounded platelets displaying some degranulation (green color) were common. Higher activation state platelets (eg, cytosol-rich, degranulated [yellow color]) were generally distributed across the thrombi, with an increased concentration at the periphery of internal vaults. Within the forming intravascular crown, rounded, high-granulation platelets (cyan) are relatively enriched, a result suggestive of low signal intensity and slow conversion between states. These patterns are shown quantitatively in supplemental Figure 1, histogram analysis, and point to the time-delayed generation of gradients in the distribution of individual activation states.

Previous SBF-SEM results indicated that puncture wound thrombi remodel and compress resulting in a smaller thrombus volume over time.[10,18] To expand on these findings at higher resolution, we mapped, qualitatively, 20 minutes after puncture thrombi (Figure 2E-F; supplemental Figure 4). As apparent from even visual inspection, there was a significant concentration of cytosol-rich, degranulated platelets (yellow) within the central, internal portion

Table 1. Platelet neighbor pairings in wild-type jugular puncture wounds (n = 3 each)

State	Blue	Cyan	Green	Yellow	Red	Sum
One1 minute after puncture						
Population, %	1.40%	18%	**38%**	36%	7%	100%
Blue with	**37%**	48%	8%	15%	1%	109%
Cyan with	1%	**31%**	38%	29%	2%	101%
Green with	0%	15%	**47%**	36%	2%	100%
Yellow with	0%	10%	29%	**56%**	5%	100%
Red with	0%	4%	10%	36%	**50%**	100%
Five minutes after puncture						
Population, %	2.00%	12%	55%	24%	3%	96%
Blue with	**15%**	23%	36%	19%	3%	96%
Cyan with	3%	**29%**	**49%**	18%	7%	100%
Green with	0%	8%	**68%**	22%	3%	100%
Yellow with	0%	5%	33%	**56%**	6%	100%
Red with	1%	9%	21%	38%	**31%**	100%
Twenty minutes after puncture						
Population, %	4.00%	13%	37%	38%	7%	100%
Blue with	**33%**	**20%**	23%	12%	13%	100%
Cyan with	**6%**	**26%**	**34%**	22%	11%	100%
Green with	1%	8%	**51%**	35%	5%	100%
Yellow with	0%	3%	26%	**64%**	6%	100%
Red with	5%	13%	26%	38%	**18%**	100%
Low to high activation state ---➤						

Table sections are color-coded to show statistically significant differences in platelet activation state neighbor pairing relative to random chance. Pairings of 2.56 standard errors of the mean or greater than random are highlighted in orange (warm color), and pairings of less than 2.56 standard errors of the mean or more are highlighted in light blue (cold color). High effect value pairings are highlighted in purple.

of each of the 3 individual thrombi (Figure 2E-F; supplemental Figure 4). In the 20-minute examples, the exposure of high-activation-state platelets to the intravascular blood flow was blocked by their interior location within the thrombus and hence rendered inaccessible to procoagulation factors within the circulation. Consistent with this, 5-color heat mapping showed the intravascular thrombus crown at 20 minutes after puncture to be rich in relatively low-activation platelets with essentially all peripherally exposed platelets being low-activation state, blue, cyan, and some green (partially degranulated); for example, see Figure 2F. Interestingly, a distinct flow-dependent difference in platelet activation state became apparent by 20 minutes after puncture (Figure 2F boxed regions; see also Figure 2A-C). The downstream portion of the crown in parallel to flow cut examples (see also supplemental Figure 4) qualitatively showed a higher number of discoid (blue) and rounded, high-granulation platelets (cyan) compared with the upstream side (Figure 2). This is an important because it indicates that at 20 minutes after puncture the thrombi continue to recruit discoid shaped platelets from the circulation, even though, as indicated by thrombus size in the frames, the thrombi were shrinking in size. Our quantitative histogram axial profiling (supplemental Figure 1) indicated a further progression in the development of platelet activation state gradients at 20 minutes after puncture.

Quantitative global trends occurring during jugular puncture thrombus maturation

To provide quantitative comparisons of global thrombus properties, we summated the abundance of scored platelets and their platelet activation state incidence. As shown in Figure 3A-B, the number of platelets per section, midthrombus, nearly doubled from 1 minute to 5 minutes after puncture and fell in number between 5 and 20 minutes after puncture. As indicated by *P* values, these numbers are sufficient to establish a trend. When paired with previous, statistically significant SBF-SEM, vEM values for volume differences between thrombi at 1, 5, and 20 minutes, we conclude that growth in platelet number per thrombus peaked at 5 minutes after puncture. Shown in Figure 3C, the global incidence of individual platelet activation states did not vary significantly over the 20-minute postpuncture period. However, as illustrated in Figure 3D and consistent with the qualitative changes in the relative distributions of platelet activation state shown in Figure 2F, a quantitative region-of-interest approach revealed strong differences in the incidence of individual platelet activation states in a 20-minute postpuncture thrombus, with the central region of interest displaying a severalfold enrichment in high-activation, degranulated platelets (yellow) relative to upstream and downstream regions.

To map near-neighbor relationships, we used XY coordinate spatial pairing to determine neighboring platelet classifications within a 2-μm radius (centroid to centroid) of any given platelet. Our null hypothesis was that neighbor pairing would be directly proportional to the frequency of any classification state. For example, platelets showing some degranulation, adherent, rounded, morphology (green) should pair randomly with each other at a frequency of 40% to 45%. Similar pairing frequencies would be expected for rounded, granulated, adherent platelets (cyan). Quantitatively, each class tended to self-associate with a frequency higher than expected (Table 1). Statistical significance relative to chance (bold face type, warm vs cold color) was validated by 2 statistical tools, z score taking a value of >2.56 as an indicator of greater than chance pairing incidence (Table 1, bolded data) and an effect score of ≥10 (purple highlight, Table 1). To identify better kinetic trends in platelet neighbor pairing, a series of 3D bar plots were generated (supplemental Figure 5). As can be seen, discoid shaped platelets (blue), representative of platelet recruitment from the bloodstream, had a high pairing frequency with each other early (1 minute) and late (20 minutes), suggestive of concentrated localized recruitment patches. Strikingly, self-association of partially degranulated platelets was highest at 5 minutes and that of fully degranulated platelets (yellow) was highest at 20 minutes, a time of little, to no, exposure of high-activation-state platelets to intravascular blood flow and any contained procoagulation factors.

Deleting the primary v-SNARE for platelet α-granule fusion produced unanticipated effects on thrombus structure

To test the effect of perturbed platelet granule secretion, we compared thrombus structure and mapping outcomes between

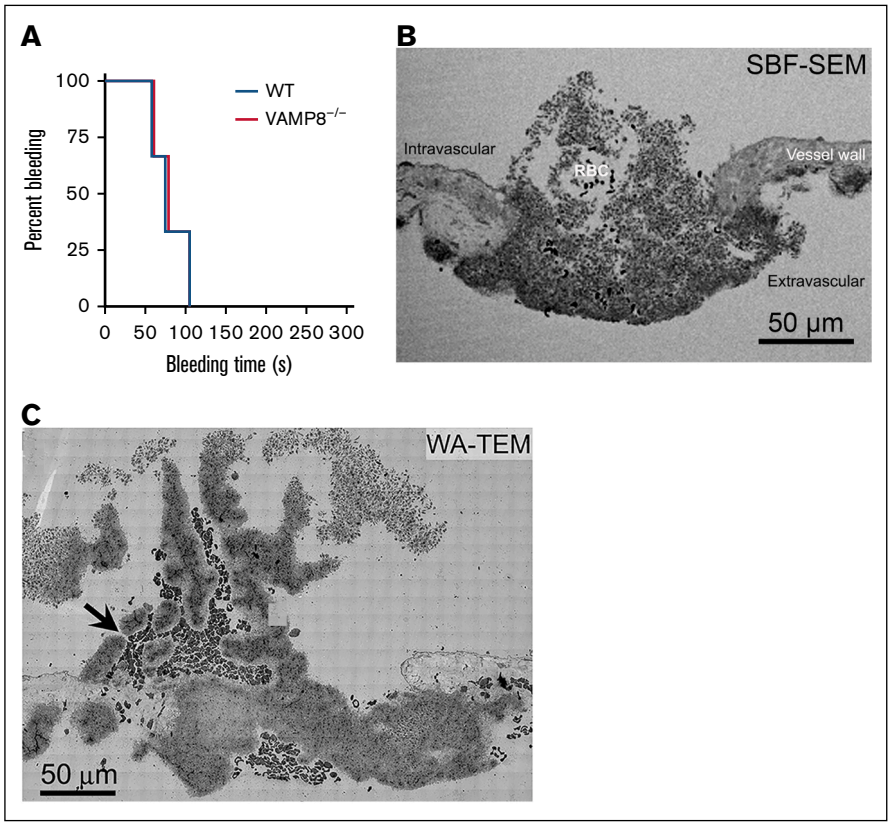

Figure 4. Deletion of VAMP8 did not affect jugular bleeding but resulted in a less organized thrombus that was porous to RBCs. (A) Bleeding time measurements in VAMP8$^{-/-}$ and WT mice after jugular puncture. (B) SBF-SEM and (C) WAT-TEM single-plane images for the resulting clot, showing its porosity to RBCs. Arrow in panel C points to RBC leakage through the porous thrombus. SBF-SEM imaging at 100 nm XY raw pixel size. WA-TEM imaging at 3.185 nm XY pixel size. RBCs are the darkest-stained cells in these images. WT, wild-type.

control and VAMP8$^{-/-}$ mice at 5 minutes after puncture. VAMP8 is the primary vesicle-soluble N-ethylmaleimide-sensitive factor attachment protein receptor (v-SNARE) implicated in α-granule fusion with the plasma membrane and its deletion slows α-granule release.[26,27] Considering the limited to no effect of VAMP8 KO on bleeding cessation in tail bleeding assays or in the jugular puncture wound model (Figure 4A), our expectation was that VAMP8 deletion should have little to no obvious effect on jugular puncture wound thrombus structure. However, SBF-SEM vEM (100-nm XY pixel size, 200-nm Z spacing) revealed narrow channels, suggesting red blood cell (RBC) leakage (Figure 4B).

As shown by WA-TEM (Figure 4C, arrow), 5-minute VAMP8 KO thrombi exhibited RBC leakage and appeared disorganized relative to the wild-type examples (Figure 2). Visually, each exhibited a cavity-filled interior with RBCs present that was open to the intravascular vessel lumen (Figure 5A-B; supplemental Figure 6). Surprisingly, each thrombus was also marked by a high level of degranulated platelets (yellow color, Figure 5A; supplemental Figure 5, 3D plots) lining peripheral surfaces that enclose less-activated interior platelets. Quantitatively, the frequency of degranulated platelets more than doubled relative to that of 5-minute wild-type thrombi (23%, control vs 57%, VAMP8 KO; Figure 5C). The increase in degranulated platelet frequency was accompanied by a decrease in the frequency of moderately activated, partially degranulated platelets (green) abundant in the thrombus interiors. Interestingly, VAMP8$^{-/-}$ had almost no effect on the number of platelets per cross-section compared with control, wild-type 5-minute thrombi (Figure 5D). As expected from the qualitative imaging, neighbor pairing frequency for highly activated platelets (degranulated, yellow; and cytosol-free, red) was high and statistically significant (Figure 5E). In conclusion, we speculate that the high level of platelet degranulation observed in the VAMP8$^{-/-}$ thrombus can be explained by SNARE fusion protein redundancy[29] and/or compensatory mechanisms, for example, exposed procoagulant surfaces.

Jugular vein and femoral artery thrombi have similar platelet activation state stratification

To test whether an arterial puncture wound shared similar platelet stratification principles to that of jugular puncture wounds, we used a 33-gauge needle (210 μm nominal diameter, 1.56-minute

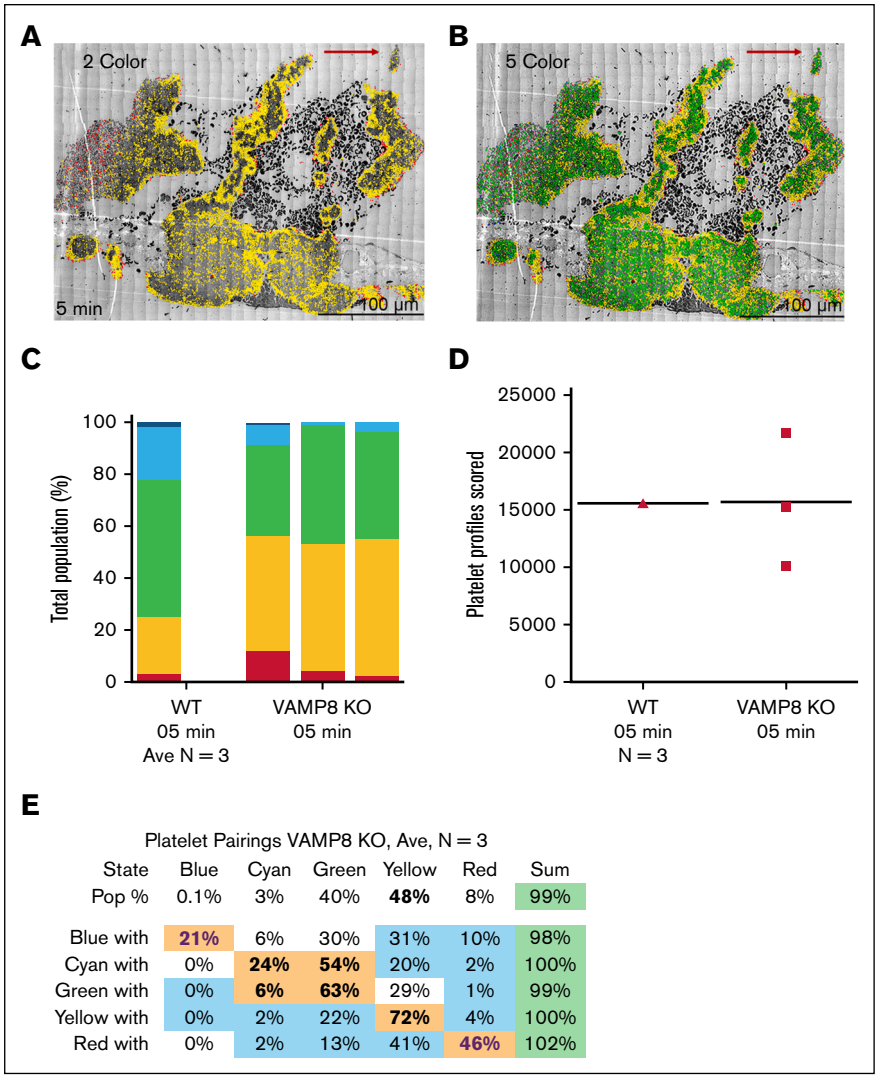

State	Blue	Cyan	Green	Yellow	Red	Sum
Pop %	0.1%	3%	40%	**48%**	8%	99%
Blue with	**21%**	6%	30%	31%	10%	98%
Cyan with	0%	**24%**	**54%**	20%	2%	100%
Green with	0%	**6%**	**63%**	29%	1%	99%
Yellow with	0%	2%	22%	**72%**	4%	100%
Red with	0%	2%	13%	41%	**46%**	102%

Figure 5. Comparative properties of 5-minute postpuncture thrombi from VAMP8$^{-/-}$ mice. (A-B) Two-color (yellow and red) and 5-color activation maps of a representative WA-TEM image of a 5-minute postpuncture thrombus from VAMP8$^{-/-}$ mice (3.185 nm XY size). RBCs are black and variably biconcave in this plane. Two additional examples are shown in supplemental Figure 3. (C) Comparative abundance of platelet activation classes showed an increased abundance of high-activation, degranulated platelets in the VAMP8$^{-/-}$ thrombi. (D) The number of platelets scored. VAMP8 loss had no significant effect on thrombus size. (E) Neighbor pairing frequencies in the VAMP8$^{-/-}$ mice showed the incidence of high-degranulation platelet self-pairing, yellow with yellow or red with red. This high incidence is consistent with the preferential localization of high-activation platelets toward exposed thrombus surfaces in the VAMP8$^{-/-}$ mice. Pairings that are 2.56 standard errors of the mean above random are highlighted in orange, whereas pairings <2.56 standard errors of the mean above random are highlighted in blue. The highest degrees of association are highlighted in purple text. Ave, average; WT, wild-type.

Figure 6. Activation state mapping of a 5-minute, postpuncture, femoral artery injury. (A-B) Two- and 5-color heat maps. (C) Platelet neighbor-pairing data. Pairings that are ≥2.56 standard errors of the mean above random are highlighted in orange, whereas pairings <2.56 standard errors of the mean above random are highlighted in blue. The highest degrees of association are highlighted in purple text. Note the strong concentration of high-activation-state platelets (yellow) on peripheral surfaces within the thrombus.

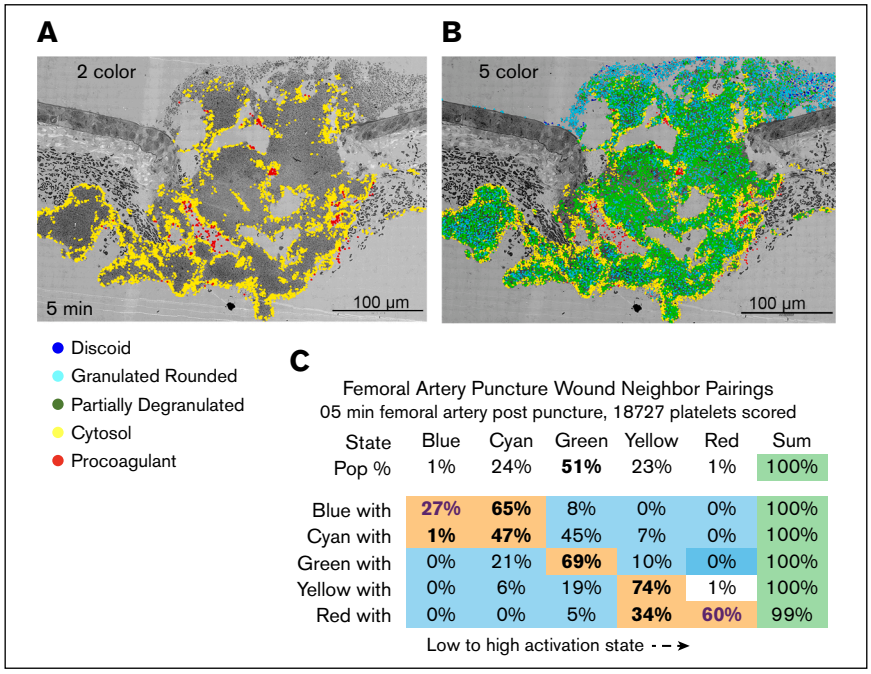

average bleeding time), to produce puncture wound examples in the femoral artery. As shown in Figure 6A-B, midthrombus WA-TEM, parallel to flow, 5-minute femoral puncture wound, the thrombus also exhibited a vaulted structure, like the jugular thrombi, in which the interior surfaces of the vaults were enriched in cytosol-positive, degranulated platelets (yellow) and highly activated platelets (red). The high degree of enrichment in highly activated platelets along the vault interior surfaces was supported by the high neighbor self-pairing frequency (yellow with yellow, Figure 6C) interior portions of the thrombus that were rich in granulated platelets (75% overall abundance, cyan and green). Peripheral regions of the intravascular crown were enriched for discoid shaped platelets and other low-activation-state platelets. As expected, the 5-minute thrombus appeared to be capped from the extravascular side. We conclude that there are several structural similarities across the 5-minute thrombi, suggesting some commonality in the mechanism of formation, regardless of flow pressures and vessel architecture. Interestingly, concentration of degranulated, high-activation platelets along the interior surfaces of the thrombi was highest for the VAMP8 KO and the femoral artery thrombi, suggestive of a possible common response to higher stress conditions, VAMP8 KO, and higher arterial flow.

Discussion

We defined the distribution of platelet activation states within a growing thrombus at the individual platelet level based on a set of morphological, ultrastructural criteria based on platelet shape, α-granule abundance, and the presence or absence of cytosol. Our expectation was that experimental outcomes in the profusely bleeding, puncture wound might reveal much more spatial complexity than the more binary core and shell[23] outcomes highlighted by previous intravital light microscopy of small, typically nonpenetrating injuries.[30,31] Our data show that a time-dependent

Figure 7. The "build and reorganize" model of thrombosis after puncture injury. Depicted are the stages of thrombosis after a puncture injury. Over the course of thrombus growth, clot reorganization and compression limit the exposure of high-activation-state platelet surfaces to the circulation and generate a thrombus displaying multiple gradients in platelet activation.

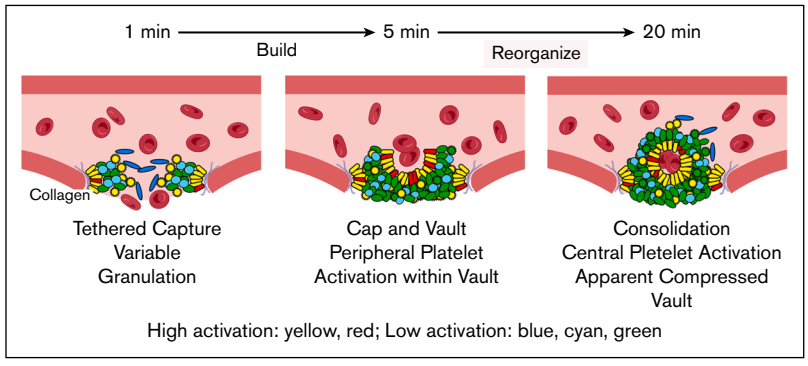

structural reorganization generated gradients in platelet activation state distribution and limited the access of procoagulant surfaces to the circulation. Loss of VAMP8, the primary v-SNARE in platelets,[26] affected the evolution of clot formation. Although there was no increase in bleeding time, our results unexpectedly showed an increased platelet degranulation in the thrombi of the VAMP8$^{-/-}$ mice. Also unexpected, the structure of the resolving thrombus, despite the morphological encapsulation of the most activated platelets (and presumably the most procoagulant), continued to exhibit significant indication of discoid platelet recruitment to the intralumenal crown. Our data clearly demonstrate the novel complexity of primary thrombosis after puncture wounding and suggest more detailed mechanistic insights into how the clot formation becomes self-limiting.

We used 2 complementary vEM techniques, WA-TEM and SBF-SEM, to visualize platelet activation and manual methodology to convert ultrastructure into maps of individual platelet activation states within forming jugular vein and femoral artery puncture wound thrombi.[10,18,24,25] Our analysis started from a 3.185-nm pixel size, which was binned to accommodate 32-bit image analysis software, an effective 12- to 15-nm size, sufficient to reveal the internal features of the thrombus and platelets in detail. We were able to perform quantitative analyses of the distribution of platelet activation states using near-neighbor state pairing, X and Y histogram profiling, and global quantification within the thrombi. We note that our resultant blinded, manual annotation serves as the ground-truth examples for our parallelly developed, 2D deep-learning artificial intelligence approach, which, combined with conventional filtering and watershed algorithms, considerably speeds the annotation and analysis steps (M. O. Faruque, K. K. Ball, and I. D. Pokrovskaya, unpublished data, November 2025).

Our quantitative data provide strong evidence that platelet heterogeneity in activation state is distributed in a near uniform manner within a 1-minute thrombus, an outcome totally unpredicted by core and shell models.[23] Platelet distributions only become nonhomogeneous, more clustered, over time, after bleeding cessation. For example, highly activated platelets in the 5-minute jugular vein or femoral artery thrombi tend to be enriched on the peripheral lining of the vaulted cavities exposed to the circulation. Physiologically, this could expose procoagulant membranes to coagulation factors and, hence, their extent of exposure could present an important regulatory step in limiting thrombus growth. We account for events that occur within large blood vessels, albeit those of mice, be they the jugular vein or the femoral artery, injured by puncture. What principles may dominate across varying physical dimensions of the thrombus and injury is an open question because smaller-diameter systems, such the extensively studied cremaster arterioles, have not been examined in depth at an equivalent resolution.[19,21,22] The data raise the need to rethink aspects of platelet-thrombus dynamics. For example, deletion of VAMP8 did not affect bleeding cessation time despite producing jugular vein thrombi that were structurally leaky to RBCs.

Paradoxically, the abundance of highly activated platelets lining the interior vaulted surfaces of 5-minute postpuncture thrombi was significantly increased in VAMP8$^{-/-}$ mice. The observed normal bleeding times could be explained, on the one hand, by SNARE fusion protein redundance.[29] On the other hand, compensatory, non–SNARE-mediated mechanisms may exist, such as the increased incidence of degranulated, highly activated platelets lining the interior surfaces of vaulted thrombus cavities at 5 minutes after puncture. Our structural studies strongly indicate bleeding cessation assays are a relatively insensitive measure. Furthermore, our data point to unexpected late-stage dynamics within the puncture wound thrombus. We had shown previously by SBF-SEM vEM that jugular puncture wound thrombi decreased in volume, presumably due to fibrin contraction.[30] Here, we show that this contraction is accompanied by a parallel decrease in platelet number. Moreover, at the same time, the data suggest that platelet recruitment to the thrombus continues. Discoid shaped platelets as those seen in the circulation were enriched in the downstream portion of the intravascular crown of the 20-minute jugular thrombus. In brief, these unanticipated dynamic aspects of thrombus formation point to the need for new models. We suggest a "build and reorganize" model (Figure 7).

Acknowledgments

The authors acknowledge that this work was a team effort spanning over several years. The authors are grateful for puncture wound samples, gifted by Timothy J. Stalker of the University of Pennsylvania, in association with Lawrence F. Brass, which made significant contributions to initiating this work.

Work at all sites was supported by the National Heart, Lung, and Blood Institute of the National Institutes of Health (NIH): University of Arkansas for Medical Sciences (NIH grants R01 HL119393, R56 HL119393, and R01 155519 [B.S.]) and subawards from NIH grants R01 HL146373 and R35 HL150818; University of Pennsylvania (NIH grants P01 HL040387 [Timothy J. Stalker]) and P01 HL120846 ([Timothy J. Stalker and Lawrence F. Brass]); University of Kentucky (NIH grant MIRA HL150818 [S.W.W.]). The Leapman laboratory was supported by the intramural program of the National Institute of Biomedical Imaging and Bioengineering at the NIH.

Authorship

Contribution: S.W.R. and I.D.P. contributed to experimental implementation with major roles in data gathering; K.K.B. was responsible for puncture wounds and all animal surgeries at the University of Arkansas for Medical Sciences (UAMS); J.A.K. supported electron microscope sample preparation and electron microscopy at UAMS; all serial block face scanning electron microscopy was done by the Leapman laboratory at National Institute of Biomedical Imaging and Bioengineering with M.A.A. and R.D.L. being major contributors to experimental design and supervision; I.D.P. led all electron microscope sample preparation and wide-area transmission electron microscopy and was responsible for data validation and coordination between the Storrie and Leapman laboratories; M.W.W. and I.D.P. were responsible for manual annotation of the images; S.W.R., R.D.L., and B.S. had major responsibilities for data quality control and manuscript preparation; B.S. wrote the first draft; E.R.D., E.S.F., and S.W.W. helped in editing the manuscript and designing some of the figures; and VAMP8-knockout mice originated in the laboratory of S.W.W. at the University of Kentucky.

Conflict-of-interest disclosure: The authors declare no competing financial interests.

ORCID profiles: I.D.P., 0009-0009-6491-3179; R.D.L., 0000-0002-8575-4084; E.R.D., 0009-0004-0483-9361; S.W.W., 0000-0001-5577-0473; B.S., 0000-0002-4644-2504.

Correspondence: Brian Storrie, Department of Physiology and Cell Biology, University of Arkansas for Medical Sciences, 4301 W Markham St, Little Rock, AR 72205; email: storriebrian@uams.edu.

References

1. Gibbins JM. Platelet adhesion signalling and the regulation of thrombus formation. *J Cell Sci*. 2004;117(pt 16):3415-3425.
2. Gawaz M, Langer H, May AE. Platelets in inflammation and atherogenesis. *J Clin Invest*. 2005;115(12):3378-3384.
3. White JG. Platelet structural physiology: the ultrastructure of adhesion, secretion, and aggregation in arterial thrombosis. *Cardiovasc Clin*. 1987;18(1):13-33.
4. Guerrero JA, Kyei M, Russell S, et al. Visualizing the von Willebrand factor/glycoprotein Ib-IX axis with a platelet-type von Willebrand disease mutation. *Blood*. 2009;114(27):5541-5546.
5. Wang JW, Valentijn JA, Valentijn KM, et al. Formation of platelet-binding von Willebrand factor strings on non-endothelial cells. *J Thromb Haemost*. 2012;10(10):2168-2178.
6. Bryckaert M, Rosa JP, Denis CV, Lenting PJ. Of von Willebrand factor and platelets. *Cell Mol Life Sci*. 2015;72(2):307-326.
7. Denorme F, Vanhoorelbeke K, De Meyer SF. von Willebrand factor and platelet glycoprotein Ib: a thromboinflammatory axis in stroke. *Front Immunol*. 2019;10:2884.
8. Thomas S. Platelet membrane glycoproteins in haemostasis. *Clin Lab*. 2002;48(5-6):247-262.
9. Kato K, Kanaji T, Russell S, et al. The contribution of glycoprotein VI to stable platelet adhesion and thrombus formation illustrated by targeted gene deletion. *Blood*. 2003;102(5):1701-1707.
10. Pokrovskaya ID, Rhee SW, Ball KK, et al. Tethered platelet capture provides a mechanism for restricting circulating platelet activation to the wound site. *Res Pract Thromb Haemost*. 2023;7(2):100058.
11. Stalker TJ, Newman DK, Ma P, Wannemacher KM, Brass LF. Platelet signaling. *Handb Exp Pharmacol*. 2012;(210):59-85.
12. Brass LF, Diamond SL. Transport physics and biorheology in the setting of hemostasis and thrombosis. *J Thromb Haemost*. 2016;14(5):906-917.
13. Shen J, Sampietro S, Wu J, et al. Coordination of platelet agonist signaling during the hemostatic response in vivo. *Blood Adv*. 2017;1(27):2767-2775.
14. Abaeva AA, Canault M, Kotova YN, et al. Procoagulant platelets form an alpha-granule protein-covered "cap" on their surface that promotes their attachment to aggregates. *J Biol Chem*. 2013;288(41):29621-29632.
15. Aliotta A, Krusi M, Bertaggia Calderara D, et al. Characterization of procoagulant COAT platelets in patients with Glanzmann thrombasthenia. *Int J Mol Sci*. 2020;21(24).
16. DeCortin ME, Brass LF, Diamond SL. Core and shell platelets of a thrombus: a new microfluidic assay to study mechanics and biochemistry. *Res Pract Thromb Haemost*. 2020;4(7):1158-1166.
17. Tomaiuolo M, Matzko CN, Poventud-Fuentes I, Weisel JW, Brass LF, Stalker TJ. Interrelationships between structure and function during the hemostatic response to injury. *Proc Natl Acad Sci U S A*. 2019;116(6):2243-2252.
18. Rhee SW, Pokrovskaya ID, Ball KK, et al. Venous puncture wound hemostasis results in a vaulted thrombus structured by locally nucleated platelet aggregates. *Commun Biol*. 2021;4(1):1090.
19. Furie B, Furie BC. Thrombus formation in vivo. *J Clin Invest*. 2005;115(12):3355-3362.
20. Dubois C, Panicot-Dubois L, Gainor JF, Furie BC, Furie B. Thrombin-initiated platelet activation in vivo is vWF independent during thrombus formation in a laser injury model. *J Clin Invest*. 2007;117(4):953-960.
21. Carminita E, Tourn J, Crescence L, et al. A thrombus is formed by a gradient of platelet activation and procoagulant endothelium. *Res Pract Thromb Haemost*. 2023;7(7):102209.
22. Celi A, Merrill-Skoloff G, Gross P, et al. Thrombus formation: direct real-time observation and digital analysis of thrombus assembly in a living mouse by confocal and widefield intravital microscopy. *J Thromb Haemost*. 2003;1(1):60-68.
23. Stalker TJ, Traxler EA, Wu J, et al. Hierarchical organization in the hemostatic response and its relationship to the platelet-signaling network. *Blood*. 2013;121(10):1875-1885.
24. Pokrovskaya ID, Ball KK, Webb MW, et al. Contrasting effects of platelet GPVI deletion versus Syk inhibition on mouse jugular vein puncture wound structure. *Int J Mol Sci*. 2025;26(9):4294.
25. Ball K, Pokrovskaya I, Storrie B. Puncture wound hemostasis and preparation of samples for montaged wide-area electron microscopy analysis. *J Vis Exp*. 2024;207.
26. Ren Q, Barber HK, Crawford GL, et al. Endobrevin/VAMP-8 is the primary v-SNARE for the platelet release reaction. *Mol Biol Cell*. 2007;18(1):24-33.
27. Pokrovskaya ID, Joshi S, Tobin M, et al. SNARE-dependent membrane fusion initiates alpha-granule matrix decondensation in mouse platelets. *Blood Adv*. 2018;2(21):2947-2958.

28. Pokrovskaya I, Tobin M, Desai R, et al. Structural analysis of resting mouse platelets by 3D-EM reveals an unexpected variation in alpha-granule shape. *Platelets*. 2021;32(5):608-617.

29. Joshi S, Prakhya KS, Smith AN, Chanzu H, Zhang M, Whiteheart SW. The complementary roles of VAMP-2, -3, and -7 in platelet secretion and function. *Platelets*. 2023;34(1):2237114.

30. Falati S, Gross P, Merrill-Skoloff G, Furie BC, Furie B. Real-time in vivo imaging of platelets, tissue factor and fibrin during arterial thrombus formation in the mouse. *Nat Med*. 2002;8(10):1175-1181.

31. Furie B, Furie BC. In vivo thrombus formation. *J Thromb Haemost*. 2007;5(suppl 1):12-17.